Rolling and aging in temperature-ramp soft adhesion

Giuseppe Boniello,[1] Christophe Tribet,[1] Emmanuelle Marie,[1] Vincent Croquette,[2] and Dražen Zanchi[1,3,*]

[1]*École Normale Supérieure, Département de Chimie, UMR CNRS-ENS-UPMC 8640 PASTEUR, 24, rue Lhomond, F-75005 Paris, France*

[2]*École Normale Supérieure, Département de Physique and Département de Biologie, Laboratoire de Physique Statistique UMR CNRS-ENS 8550, 24, rue Lhomond, F-75005 Paris, France*

[3]*Université de Paris 7 Denis Diderot, 5 rue Thomas Mann, 75013 Paris, France*

(Received 3 September 2017; published 17 January 2018)

Immediately before adsorption to a horizontal substrate, sinking polymer-coated colloids can undergo a complex sequence of landing, jumping, crawling, and rolling events. Using video tracking, we studied the soft adhesion to a horizontal flat plate of micron-size colloids coated by a controlled molar fraction f of the poly(lysine)-grafted-poly(N-isopropylacrylamide) (PLL-g-PNIPAM) which is a temperature-sensitive polymer. We ramp the temperature from below to above $T_c = 32 \pm 1°C$, at which the PNIPAM polymer undergoes a transition, triggering attractive interaction between microparticles and surface. The adsorption rate, the effective in-plane (x-y) diffusion constant, and the average residence time distribution over z were extracted from the Brownian motion records during last seconds before immobilization. Experimental data are understood within a rate-equations-based model that includes aging effects and includes three populations: the untethered, the rolling, and the arrested colloids. We show that preadsorption dynamics casts a characteristic scaling function $\alpha(f)$ proportional to the number of available PNIPAM patches met by soft contact during Brownian rolling. In particular, the increase of in-plane diffusivity with increasing f is understood: The stickiest particles have the shortest rolling regime prior to arrest, so that their motion is dominated by the untethered phase.

DOI: 10.1103/PhysRevE.97.012609

I. INTRODUCTION

Adhesion of colloids on a flat surface presents interesting aging dynamics if either of the surfaces is elastic or soft [1]. Soft adhesion with aging dynamics can also be produced by coating surfaces with a polymer whose ends can stick to the adjacent surface, as has been recently reported [2]. During soft adhesion, ends of polymers protruding from engaged surfaces stochastically explore the opposite side, increasing the number of attached contacts, so that the soft contact domain evolves in time. Control of these very final events preceding the immobilization are of interest for research on functional materials, lubrication, cell adhesion, etc. [3–6]. In the present paper, we focus on colloids coated by a controlled molar fraction f of T-responsive polymers that switch interactions between colloids and the surface from repulsive to attractive at $T = T_c \approx 32°C$. We analyze the details of the colloid Brownian motion occurring just before their adsorption to the surface. Near-surface Brownian dynamics can be analyzed by direct video two-dimensional (2D) or three-dimensional (3D) tracking, either by real-time analysis of the diffraction pattern [7,8], by total internal reflection microscopy (TIRM) [9–11], or by three-dimensional ratiometric total internal reflection fluorescence microscopy (3D R-TIRFM) [12,13]. The mean-square displacement (MSD) reveals how the diffusion is hindered by near-surface effects [14–17]. In the 3D tracking, the resident time distribution (RTD), corresponding to the z histogram of the trajectory, has been used for studying the particle-surface interaction potential [11]. If the adsorption (or self-aggregation) is irreversible, as it is in our present case, the situation is clearly an out-of-equilibrium process. In such a case, the aging effects in the preadhesion phase were identified in constant shear flux by Kalasin and Santore [2] and for a particle held (and released) by optical tweezers in suspension above a flat surface, by Kumar *et al.* [1,18]. To bring the system out from equilibrium we use T-switchable attraction between colloids and the surface. Namely, T responsiveness of the polymer poly(N-isopropylacrylamide) (PNIPAM, $T_c = 32 \pm 1°C$ [19]), at varying surface molar fraction f, was already exploited for analysis of self-association kinetics of coated microparticles [20,21].

In the experimental section of the paper, we present methods and results. The theoretical section reports on a simple adsorption model, allowing to understand all experimental findings. Several issues that our results and their interpretation could raise are pointed out in the discussion section. The final section contains concluding remarks.

II. EXPERIMENTAL SECTION

A. Materials and methods

Silica beads (0.96 μm in diameter, Bangs Laboratories, SS03N) are dispersed in sodium hydroxide solution 1M by sonication for 15 min and dialysed against water (Slide-A-Lyzer, M_W cutoff 3500 kDa, Thermo Scientific). The solution is diluted in phosphate-buffered saline (PBS) solution (0.15 M). Particle coating is obtained by mixing 22 μL of beads in PBS with 100 μL of polymer solution 10 $g\,L^{-1}$ [f% poly(lysine)-grafted-poly(N-isopropylacrylamide) (PLL-g-PNIPAM),

*zanchi@ens.fr

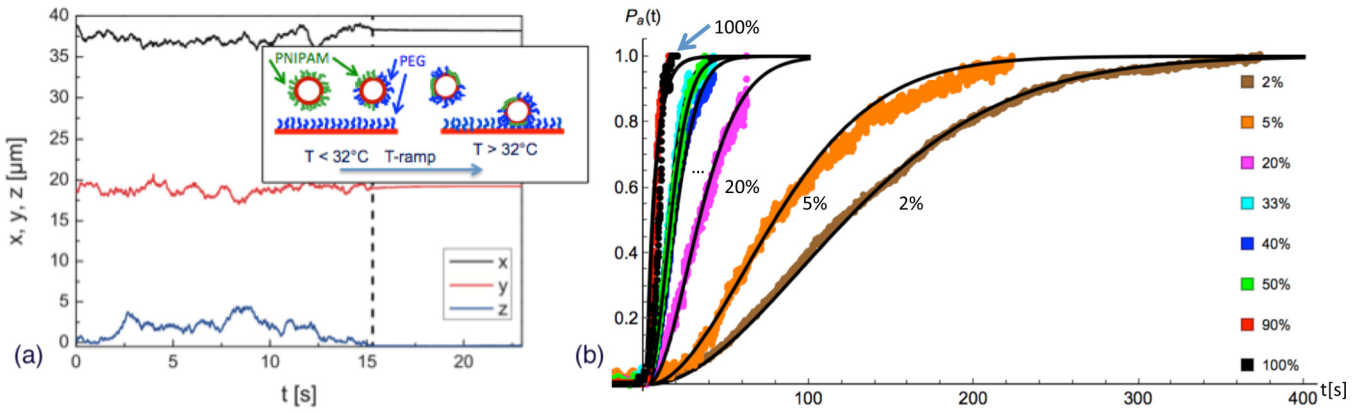

FIG. 1. (a) Typical 3D tracking record. Bead was captured irreversibly at $t = 15.2$ s. Inset: schematic visualization of temperature ramp experiment. (b) Fraction of adsorbed particles as a function of time in a T ramp of 10°C/min between 26 and 38°C, for a range of PNIPAM ratios f. Solid lines are calculated best fitting adsorption profiles $P_a(t)$.

$(100 - f)\%$ poly(lysine)-grafted-polyethyleneoxide (PLL-g-PEG), PLL $M_w = 15$–30 kg/mol, PEG $M_w = 20$ kg/mol, PNIPAM $M_w = 7$ kg/mol] in PBS. The resulting suspension is incubated for 30 min at room temperature. Polymer excess is removed by five centrifugation cycles (1800 g for 5 min), replacing the supernatant by deionized water.

To create the flat substrate, borosilicate glass cover slips are cleaned with ethanol and plunged in a 1M sodium hydroxide ultrasonic bath for 30 min. After rinsing with deionized water and drying, the experimental cell is prepared by superposing biadhesive tape and a mylar film. A 52 mm x 5 mm x 50 μm channel is thus created between the borosilicate glass slide and the mylar film. The bottom of the channel is functionalized by coating the glass surface with PLL-g-PEG (same as the one used for coating particles), ensuring a steric repulsion for $T < T_c$. This is achieved by injecting polymer solution (1 gL^{-1} in PBS) in the cell and incubating for 30 min at room temperature. The cell is then rinsed with deionized water and dried by compressed air.

In the T-ramp experiment, the particle suspension is injected in the cell at 26 °C, and the temperature is increased at 10 °C/min up to 38 °C and is kept constant until the end of the acquisition. Attraction between beads and the flat plate is thereby triggered by crossing the critical temperature $T_c = 32 \pm 1$°C. The advantage of the method is twofold. First, it allows us to switch from repulsive to attractive regimes without requiring fine temperature control around the transition temperature. Second, we get rid of additional effects, such as thermal inertia or uncertainty on PNIPAM transition. The 3D bead motion is observed by slightly defocused microscopy in parallel illumination, decorating the bead image with interference rings observed with a video camera (UI-3060CP with 2.3 MP sensor IMX174, 1936 x 1216 px, Sony). Particles are tracked in real time using a PicoTwist apparatus and PICOUEYE software [7], allowing subpixel resolution (∼5 nm) at 50 frames/s; see Fig. 1(a).

To measure the fraction of adsorbed particles over time, large number of particles (typically 40–50 per run) are followed by a charged-coupled device (CCD) camera at 10 frames/s, as long as all visible beads are immobilized. The recorded movies are converted to binary masks (1, particle; 0, background). Cumulative distributions of binding times, i.e., the fraction of adsorbed particles, are extracted from the correlation of each frame with the last one,

$$P_a(t) = \frac{\sum_{x,y} I(t) I(t_f)}{\sum_{x,y} I(t_f)}, \tag{1}$$

where $\sum_{x,y}$ stands for the sum of all the pixel values on the same resulting image.

At a given coverage ratio f, the in-plane average diffusion $D_{\rm eff}(f)$ is obtained by fitting the mean-square displacement (MSD) extracted from in-plane tracking over the final time interval $[t_0 - \Delta t, t_0]$ before stopping at $t = t_0$. In our experiment $\Delta t = 16$ s was chosen: long enough to contain several up-down excursions and short enough to give meaningful results even for rapidly adsorbing particles. The MSD for the ith particle on stage is extracted from $x_i(t)$ and $y_i(t)$ tracks using the relation

$$\mathrm{MSD}_{x,i} \equiv \langle [x_i(t + t') - x_i(t')]^2 \rangle_{t'} = 2 D_{\mathrm{eff},i}\, t, \tag{2}$$

and equivalently for MSD_y. The average $\langle \cdots \rangle_{t'}$ runs over t', lying within the observed time interval Δt. For all values of f, MSDs are linear in time over several seconds, indicating that the movement is diffusive. The diffusion constant is obtained by fitting Eq. (2) for each of typically $N \sim 10$ particles per run and taking the average: $D_{\rm eff} = \langle D_{\mathrm{eff},i} \rangle_i$.

Finally, for each 3D track, the RTD over z direction is extracted by constructing histogram of the z track record within typically 6–7 μm above the flat surface, and averaged over N particles from the same run.

B. Results

The fraction of immobilized particles as function of time is shown in Fig. 1(b). Samples with higher PNIPAM coverage f adsorb faster. The characteristic sigmoidal shape of the adsorption kinetics indicates that adsorption rate increases gradually, corroborating the aging nature of the preadhesion dynamics of surface engaged particles.

If particles are in contact with the surface and rolling (or crawling) most of the time, their in-plane average diffusion $D_{\rm eff}$ is reduced, as observed in experiments with finely thermostated DNA-coated microbeads [17]. Our systems

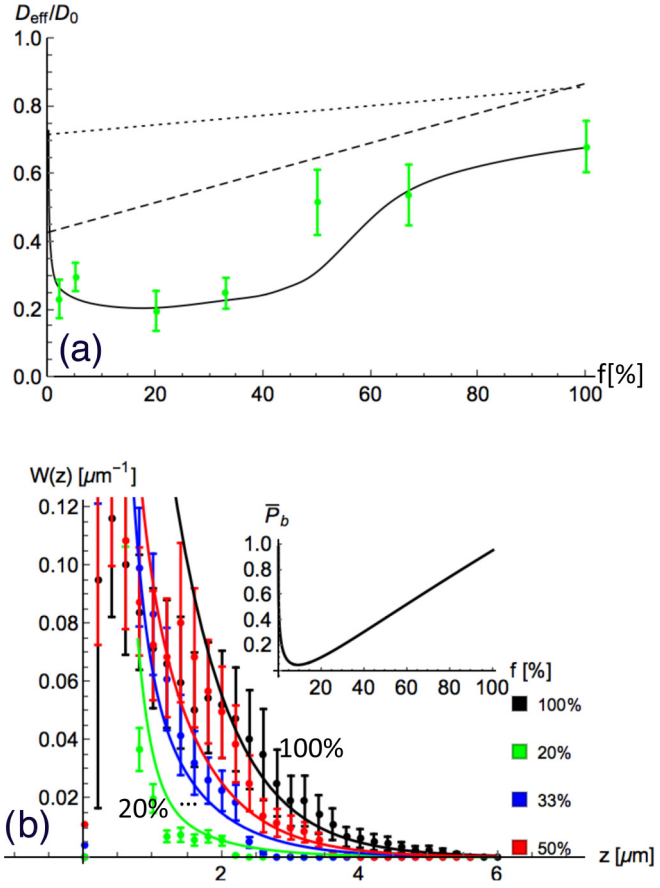

FIG. 2. (a) Experimental points: effective in-plane diffusion $D_{\text{eff}}(f)$ obtained by fitting the MSDs immediately before stopping. Bold line: result of our theory. Dotted lines: estimation of the near-wall diffusion hindrance by hydrodynamic effects near partially absorbing wall in gravitational potential. Dashed line: same estimation, including van der Waals potential. (b) Residence time distribution (RTD) extracted from tracking records $z(t)$ record, compared to calculated PDF $W(z)$. Inset: $\bar{P}_b(f)$, the calculated average time fraction that particles spend away from the surface during the recording time interval.

shows similar behavior. Figure 2(a) shows $D_{\text{eff}}(f)/D_0$, where $D_0 = k_BT/6\pi\mu R = 0.67\ \mu\text{m}^2/\text{s}$ is the diffusion constant for 1-μm beads in water far from wall at 38°C. As we increase f from 2% to 100%, D_{eff}/D_0 increases from ~0.2 to ~0.65. Naively, one would expect the opposite, that is, the particles are slower as their stickiness is higher. As we will show in the next section, the puzzle is solved by assuming that the surface-engaged beads are much slower than the untethered ones and that the time that beads spend in contact with the surface decreases as f increases. In fact, beads with high coverage stick rapidly after engagement, while these with low f spend most of their time rolling, which lowers their diffusion coefficient considerably.

The normalized RTD over z is shown on Fig. 2(b), as extracted from the z-record histogram. It shows that the beads with high f spend most of their pre-arrest time away from surface, while beads with lower coverage f can roll and tumble without sticking, implying that on average they spend more time closer to the surface.

III. THEORY

According to the theory of Mani, Gopinath, and Mahadavan (MGM) [22], a typical time scale for soft contact aging is given by

$$\tau^* \sim \frac{a}{l_1} \times \tau_{\text{visc.}} \times \frac{1}{2}\mathcal{K}l_1^2/k_BT, \tag{3}$$

where $\tau_{\text{visc.}} = 3\mu/(n\mathcal{K}l_1)$ is the viscous settling time, a is the microparticle radius, $\mathcal{K}$ is the spring constant of a single polymer involved in sticking, l_1 is its rest length, μ is the viscosity, and n is the number of available sticky polymer tethers per unit surface. Thus, τ^* is the result of interplay between viscoeleastic time and the attachment efficiency measured by the $\mathcal{K}l_1^2/(2k_BT)$ factor. The resulting $\tau^* = \mu a/nk_BT$ is independent of the elastic constant of the tethers. On the contrary, the settling vertical distance during the draining does depend on spring constant. However, the latter does not intervene in our present model. For our case, the most important is the inverse proportionality between τ^* and n. Notice that the binding energy per sticking tether does not enter in the MGM theory since the polymer-substrate sticking rate is determined by the first passage time. Moreover, according to [1,2,18], the prearrest dynamics of soft adhesion proceeds stepwise; i.e., the 3D approach is well separated from soft contact (2D) rolling phase, indicating that the untethered and the rolling colloids can be seen as separated populations.

We construct the rate equations for three fractions: (1) the untethered fraction represented by the probability $P_b(t)$, (2) the fraction of rolling colloids of age τ, whose probability to be found between the ages τ and $\tau + d\tau$ is $P_r(t,\tau)\,d\tau$, and (3) the population of colloids in arrest, with the probability

$$P_a(t) = 1 - P_b(t) - \int_0^t P_r(t,\tau)d\tau. \tag{4}$$

The time zero is chosen to coincide with the onset of the attractive interactions. Consequently, rolling particles cannot be older than t. To describe properly the evolution of the rolling population, we introduce following physical quantities: the sedimentation rate κ, the redesperion rate function $a(\tau)$, and the irreversible stopping rate function $b(\tau)$. κ corresponds to the fraction of particles within the observation window absorbed per unit time by a totally absorbing sink at $z = 0$. It can be determined from the stationary solution of the Fokker-Planck equation with z-dependent viscous drag due to near-wall hydrodynamic corrections [23] in gravitational and van der Waals potential. The observation window in our case corresponds to the layer of 6–7 μm above the surface. For our choice of parameters, we calculated the theoretical value $\kappa = 0.17\ \text{s}^{-1}$. $a(\tau)$ is the redispersion rate of rolling colloids of age τ back into bulk, and $b(\tau)$ is the irreversible stopping rate of rolling colloids of age τ.

The rate equation for $P_r(t,\tau)$ is determined by rates κ, $a(\tau)$, and $b(\tau)$ as follows:

$$\frac{dP_r(t,\tau)}{dt} = -\frac{\partial P_r(t,\tau)}{\partial\tau} + \delta(\tau)\kappa P_b(t) - a(\tau)P_r(t,\tau) - b(\tau)P_r(t,\tau)\,, \tag{5}$$

where $\delta(\tau)$ is Dirac function, ensuring that any newly sunk particle is a "just born" rolling one ($\tau = 0$). The first term on the right-hand side reproduces simple uniform time evolution. To illustrate, suppose that we have some initial distribution $P_r(t = 0,\tau) = F(\tau)$; in the absence of any source or sink terms ($\kappa = 0$ and $a = b = 0$ respectively) at some later time t the solution is $F(\tau - t)$, that is, the time evolution is trivial shifting by $-t$. Nontrivial (and interesting) modulation in the time evolution is brought in by sources and sinks.

The rate equation for untethered colloids is

$$\dot{P}_b = -\kappa P_b + \int_0^t a(\tau) P_r(t,\tau)\, d\tau, \tag{6}$$

which, together with Eqs. (4) and (5), determines completely the evolution of the system.

Since in our experiment the particles are unresolved over τ, starting from Eq. (5) a simplified equation is derived, in which all rolling particles are represented by

$$P_r(t) \equiv \int_0^t P_r(t,\tau) d\tau. \tag{7}$$

We will suppose that the redispersion rate $a(\tau)$ and the arrest rate $b(\tau)$ depend on τ over characteristic aging time scale τ^*, allowing us to write

$$a(\tau) = k_{\text{off}} \Phi(\tau/\tau^*),\ b(\tau) = k\chi(\tau/\tau^*), \tag{8}$$

where Φ is a monotonically decreasing and χ monotonically increasing function limited between 0 and 1. We introduce the effective aging functions ρ and g as follows:

$$\int_0^t \Phi(\tau/\tau^*) P_r(t,\tau) d\tau = \rho(t/\tau^*) P_r(t) \tag{9}$$

and

$$\int_0^t \chi(\tau/\tau^*) P_r(t,\tau) d\tau = g(t/\tau^*) P_r(t). \tag{10}$$

These relations are purely formal and do not allow us to obtain functions ρ and g from the original aging functions a and b. In this regard, the present theory is merely a phenomenology because the aging functions are not given explicitly in terms of the parameters of the model. However, the relations (9) and (10) show that it is always possible to recast the system of rate equations for $P_r(t,\tau)$ to the system for the total number of rolling beads $P_r(t)$ and that the effective aging functions ρ and g vary at the same aging time scale τ^* as the original functions a and b. By integrating over τ, Eq. (5), and using the definition (7), we obtain the rate equations

$$\begin{aligned} \dot{P}_b &= -\kappa P_b + k_{\text{off}}\, \rho(t/\tau^*) P_r, \\ \dot{P}_r &= \kappa P_b - [k_{\text{off}}\, \rho(t/\tau^*) + k\, g(t/\tau^*)] P_r, \end{aligned} \tag{11}$$

while the third population of colloids is in arrest, $P_a(t) = 1 - P_b(t) - P_r(t)$.

According to Refs. [2,18,22], the age can be associated with the number of stuck point contacts within the engaged soft domain. We chose $\rho(x) = e^{-x}$ and $g(x) = 1 - \rho(x)$ because we want the redispersion rate to decrease and the arrest rate to increase upon aging. Initial conditions of the systems are $P_r(0) = P_a(0) = 0$ and $P_b(0) = 1$. The central issue of this work is to find out how the parameters of the model, Eqs. (11), depend on f. Following MGM, we suppose that the aging time τ^* scales as n^{-1}, but with extended meaning of n as the effective surface density of sticky tethers visited by the contact domain during rolling, Fig. 3(b). Sticky tethers for us are the dangling polymers that are able to reach the opposite bare surface by overcoming the steric shield. This is possible in the immediate vicinity of the spots containing collapsed PNIPAM. The effective number of available sticky tethers is therefore proportional to the number of PNIPAM spots visited by the contact domain. For low f, we expect that average width of the contact domain is wider than typical distance between PNIPAM spots. The number of tethers involved is proportional to the linear density of PNIPAM patches along the rolling path, i.e., $n \sim f^{1/2}$, while for higher f, n becomes proportional to f, since the interpatch distance becomes smaller than the width of the searching trail. Notice that the present argumentation does not prejudice details of PNIPAM disposition over the surface, as far as PLL-g-PNIPAM is disposed in a discrete number of spots. In particular, the PLL-g-PNIPAM molecules can be grouped in patches with some size distribution. In order to confirm that present argumentation makes sense, we assumed that all parameters of Eq. (11) depend on f over a single, monotonically increasing, scaling function $\alpha(f)$, proportional to the number of available tethers within the searching area. Accordingly, for the aging time we pose $\tau^* = \tau_0^*/\alpha(f)$. Since the stopping rate constant k is supposed to increase with $\alpha(f)$, we put $k = k_0\alpha(f)$. Detachment rate constant should decrease with increasing number of sticking points: We use $k_{\text{off}} = k_{\text{off0}}/\alpha(f)$. Calculated $P_a(t)$ using Eqs. (11) are fitted to adsorption kinetics by adjusting solely the value of α for each f; see Fig. 1(b). The absolute scale for α being arbitrary, we choose $\alpha(f = 2\%) = 1$. The fitting parameters are $k_0 = k_{\text{off0}} = 0.05\ \text{s}^{-1}$ and $\tau_0^* = 350$ s for all curves. Figure 3(a) shows the best fitting scaling function $\alpha(f)$. It is consistent with $\sim\sqrt{f}$ tendency for low f and is steeper for high f, which confirms our picture based on interplay between the discreteness of PNIPAM spots and the finite width of contact domain.

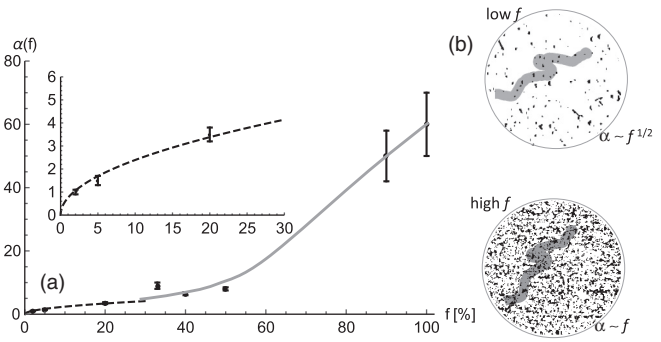

FIG. 3. (a) Dotted symbols: scaling parameter $\alpha(f)$ fitting the experiments. Low-f and high-f regimes are visible. (b) Schematic interpretation of the two regimes. Shaded trail is the bead surface portion visited by the contact domain during Brownian rolling. At low f, the number of tethers involved is proportional to the linear density of PNIPAM patches along the rolling path, while at high f it crosses over to the surface density.

We want now to reproduce the measured in-plane diffusion D_{eff}, Fig. 2(a). Since the process is nonstationary and

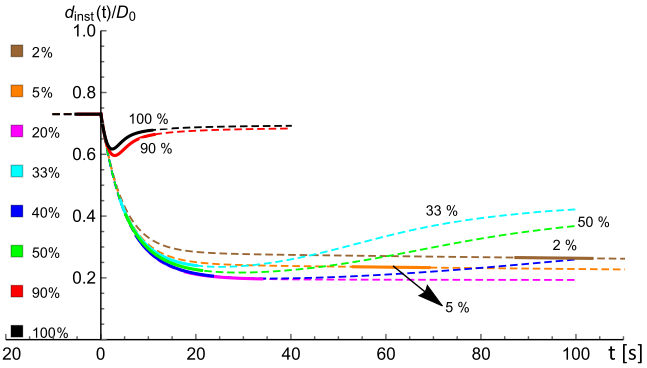

FIG. 4. Dashed line: $d_{inst}(t)/D_0$ within the present model based on aging rolling particles, for a range of coverages f. Values of $\alpha(f)$ used here are the ones that fit the adsorption kinetics, Fig. 1(b). Bold line: most probable time intervals of particle tracking. The effective diffusion constant D_{eff} is obtained as average over the bold portions; see Eq. (12).

irreversible, we must know in what moment (t_1) and for how long (Δt) the tracks are recorded, so that the average fraction of time that beads spend in "b" and in "r" state evolves in time. We assume that the most probable time t_1 is equal $t_{max}(f)$, the time of maximal adsorption rate, corresponding to the maximum slope of kinetics, Fig. 1(b). The tracking duration was $\Delta t = 16$ s, a compromise regarding the number of particle excursions between "b" and "r" and the lifetime of the moving particle starting from $t = 0$. D_{eff} is calculated as the time average of instantaneous diffusion $d_{inst}(t)$ over Δt centered at t_{max}, which mimics the way in which experimental D_{eff} is extracted from the tracking. Formally, it is written

$$D_{eff} \approx \frac{1}{\Delta t}\int_{t_{max}-\Delta t/2}^{t_{max}+\Delta t/2} d_{inst}(t)\,dt, \tag{12}$$

where the instantaneous diffusion constant is $d_{inst}(t) = [D_b P_b(t) + D_r P_r(t)]/[P_b(t) + P_r(t)]$, D_b and D_r are effective diffusion constants for untethered and rolling particles respectively, while $P_b(t)$ and $P_r(t)$ are calculated by Eqs. (11). It is important not to confound the quantity $d_{inst}(t)$ with the instantaneous diffusion "constant" of a single particle that can be extracted from the tracking and is a quickly fluctuating quantity. In fact, $d_{inst}(t)$ is interpreted as the ensemble average of diffusion constant at the time t.[1]

Calculated time evolution of $d_{inst}(t)$ for a range of coverage values f is shown by dashed lines in Fig. 4. The portions drawn in bold correspond to the most probable time intervals of tracking recording. According to Eq. (12), the resulting effective in-plane diffusion constant D_{eff} is the average over these intervals. Notice that for the very highest values of f, the acquisition interval runs partially over times $t < 0$, i.e. before the PNIPAM collapse transition at $t = 0$.

[1]Equation (12) ignores the temperature variation within the observed T-ramp segment. Namely, the temperature dependence enters via $D_0(T) = k_B T/6\pi\mu(T)R$ and $\mu(T)$ decreases from 0.77 to 0.68 mPa s between $T = T_c = 32°$C and the final temperature $T = 38°$C. The effect is neglected since it can affect only the fastest kinetics and only by a few percent, which is less than experimental inaccuracy.

The resulting calculated profile of $D_{eff}(f)/D_0$, shown in Fig. 2(a), is fitted to experimental data by adjusting D_b and D_r, while we used the same dependence $\alpha(f)$ [Fig. 3(a)] that fits the adsorption kinetics, Fig. 1(b). Best fitting values are $D_b = 0.73D_0$ and $D_r = 0.15D_0$.

In order to fit the residence time distribution (RTD), Fig. 2(b), to our theory, we associate the RTD to the probability distribution function (PDF), supposed to have the form

$$W(z) = \bar{P}_b W_b(z) + (1 - \bar{P}_b)W_r(z), \tag{13}$$

where $\bar{P}_b$ is the average $P_b(t)$ over the observation time of Δt centered at $t = t_{max}$:

$$\bar{P}_b = \frac{1}{\Delta t}\int_{t_{max}-\Delta t/2}^{t_{max}+\Delta t/2} \frac{P_b(t)}{P_b(t) + P_r(t)}\,dt. \tag{14}$$

It is in fact the average fraction of time that particle spends away from the surface during the recording time interval. We take the equilibrium barometric law for PDF of detached particles

$$W_b(z) \sim e^{-\tilde{m}gz/k_B T}, \tag{15}$$

where $\tilde{m}$ is the buoyant mass, and we assume that rolling particles have a phenomenological distribution

$$W_r(z) \sim e^{-a_r z/k_b T}, \tag{16}$$

with a_r being the apparent weight of rolling particles, $a_r \gg \tilde{m}g$. Calculated distributions $W(z)$ are shown in Fig. 2(b), together with $\bar{P}_b(f)$ in inset. We see that in the asymptotic part of RTD, corresponding to the untethered particles, is fairly well reproduced by our model; i.e., the untethered population decreases as predicted, with decreasing f.

IV. DISCUSSION

In the light of rate-equations-based theory, Eq. (11), we understand why the sample with the highest f also has the highest D_{eff}. At high f, a large majority of moving particles are in the suspension far from the surface during tracking, because the rolling regime is very short (i.e., the stopping is faster than the free sedimentation $k \gg \kappa$, so that the beads get arrested as soon as they touch the surface); see inset of Fig. 2(b). For low f, this is not the case any more: The beads spend most of their time engaged in rolling motion, which is much slower. In that sense, the most interesting regime for us is the one of moderately low f, since the rolling and aging are the signatures of soft adhesion. For $f \lesssim 5\%$, the theory predicts a rapid increase in $D_{eff}(f)/D_0$ with decreasing f, as expected, because particles without PNIPAM never stick nor roll on the surface. This regime is controlled by stopping rates constant k, which scales as $\sqrt{f}$ for small f. The points measured at $f = 5\%$ and 2% confirm this tendency.

Another instructive point to discuss concerns the value of $D_b = 0.73D_0$ that fits experimental data. One expects it to correspond to the equilibrium near-wall hindered diffusion of untethered particles. The corresponding stationary PDF taking only gravitational potential is $W_b(z)$, given by Eq. (15), which indeed fits the RTD: see Fig. 2. The diffusion constant at distance z for parallel (in-plane) motion is $D_0/\phi_\parallel(z)$, where $\phi_\parallel(z)$ is the hinderance factor due to hydrodynamic interactions of spherical particle moving near a flat surface. Analytic form of $\phi_\parallel(z)$ is a standard result, reported in the literature [24–26].

Taking average over z, we get

$$D_b = D_{\text{eff}} \mid_{f=0} = D_0 \int \frac{W_b(z)}{\phi_{\parallel}(z)} dz = 0.72 D_0, \qquad (17)$$

which is fairly close to the value that fits the experimental results.

Interestingly, taking into account also the van der Waals (vdW) interaction, we get $D_b = 0.44 D_0$, which is too low. This indicates that untethered colloids live in gravitational potential only, since the steric shield prevents them from approaching the surface and feeling the vdW forces.

One could wonder if our whole interpretation in terms of rolling and aging is overcomplicated, and that experimental findings could be understood by effects of concentration depletion in the vicinity of partially absorbing sink at $z = 0$, and casting only two populations, the untethered and the arrested ones. Indeed, it sounds plausible that higher adsorption implies lower concentration near the surfaces, and consequently some shift of the overall population upward, where diffusion hinderance is less effective. A consequence is that the average $D_{\parallel}$ increases with increasing f, just as we want. For that reason, we calculated $D_{\parallel}$, which under present assumptions equals D_b, given by Eq. (17). Calculations of $W_b(z)$ for partially absorbing wall imply finite flux solution of the Fokker-Planck equation [15]. We find that D_{eff} increases linearly with f, as shown in Fig. 2(a). Cases with gravitational potential alone and including also the van der Waals part are both in disagreement with the experimental points, which show that the model that ignores the possibility of rolling cannot explain $D_{\text{eff}}(f)$.

For a similar system, the increase of D upon raising temperature above T_c has been reported in Ref. [27] in equilibrium conditions, where the phenomenon was attributed to electrostatic effects. This interpretation cannot be applied to our case in which, for high f, the particles spend most of their time away from the surface, at distances much higher than the Debye length.

Finally, let us discuss the assumption made in our model that the f dependence is contained simply in the parameter $\alpha(f)$ with the meaning of the effective surface density of available sticking tethers during the soft sticking. This assumption assumes that individual "stick" and "release" events between one PEG end and the adjacent surface are independent of PNIPAM coverage f. In another words, when collapsing at T_c, PNIPAM patches simply allow a finite number of PEGs to reach the adjacent surface, without affecting the sticking event of each PEG with the surface, which includes the diffusive search of the surface by the PEG end. *A priori*, this is a reasonable assumption because within the PLL-g-PEG coating the surface density of PEG chains is well below the overcrowded coverage [6], which would affect the sticking and release dynamics per PEG chain at low f. The agreement between the model and the experimental findings confirms that the present interpretation makes sense.

V. CONCLUSION

In conclusion, the soft adsorption kinetics depends on f over a single function $\alpha(f)$, which is a measure of the number of discrete sticky patches within the soft contact area during Brownian rolling, extending the theory of Mani *et al.* [22]. At low and high f, the effective interpatch distance is larger and smaller than the contact diameter. From the point of view of PNIPAM spots [Fig. 3(b)], the trail of the rolling contact domain crosses over from 1D to 2D, implying crossover of $\alpha(f)$ from $\sim\sqrt{f}$ to $\sim f$. Two most remarkable effects are (i) a characteristic sigmoidal profile of the adsorption kinetics due to aging and (ii) a decrease of the in-plane diffusion constant in prearrest Brownian dynamics with decreasing f due to reduction of preadhesion rolling time.

ACKNOWLEDGMENTS

We thank M. Nobili for a critical reading of the manuscript and K. Sekimoto for stimulating and helpful discussions. This work was funded by Agence Nationale de la Recherche: ANR-13-BS08-0001-01 (DAPPlePur) and ANR-11-LABX-0011-01 (program "investissement d'avenir").

[1] P. Sharma, S. Ghosh, and S. Bhattacharya, Nat. Phys. **4**, 960 (2008).
[2] S. Kalasin and M. M. Santore, Macromolecules **49**, 334 (2015).
[3] Y. Wang, Y. Wang, X. Zheng, É. Ducrot, J. S. Yodh, M. Weck, and D. J. Pine, Nat. Commun. **6**, 7253 (2015).
[4] M. A. C. Stuart, W. T. Huck, J. Genzer, M. Müller, C. Ober, M. Stamm, G. B. Sukhorukov, I. Szleifer, V. V. Tsukruk, M. Urban *et al.*, Nat. Mater. **9**, 101 (2010).
[5] J. C. Crocker, Nature (London) **451**, 528 (2008).
[6] S. Gon, K.-N. Kumar, K. Nüsslein, and M. M. Santore, Macromolecules **45**, 8373 (2012).
[7] C. Gosse and V. Croquette, Biophys. J. **82**, 3314 (2002).
[8] G. Boniello, C. Blanc, D. Fedorenko, M. Medfai, N. B. Mbarek, M. In, M. Gross, A. Stocco, and M. Nobili, Nat. Mater. **14**, 908 (2015).
[9] D. C. Prieve, Adv. Colloid Interface Sci. **82**, 93 (1999).
[10] S. Behrens, J. Plewa, and D. Grier, Eur. Phys. J. E **10**, 115 (2003).
[11] H.-J. Wu and M. A. Bevan, Langmuir **21**, 1244 (2005).
[12] K. Kihm, A. Banerjee, C. Choi, and T. Takagi, Exp. Fluids **37**, 811 (2004).
[13] C. Choi, C. Margraves, and K. Kihm, Phys. Fluids **19**, 103305 (2007).
[14] L. P. Faucheux and A. J. Libchaber, Phys. Rev. E **49**, 5158 (1994).
[15] M. A. Bevan and D. C. Prieve, J. Chem. Phys. **113**, 1228 (2000).
[16] P. Sharma, S. Ghosh, and S. Bhattacharya, Appl. Phys. Lett. **97**, 104101 (2010).
[17] Q. Xu, L. Feng, R. Sha, N. C. Seeman, and P. M. Chaikin, Phys. Rev. Lett. **106**, 228102 (2011).
[18] D. Kumar, S. Bhattacharya, and S. Ghosh, Soft Matter **9**, 6618 (2013).

[19] O. J. Cayre, N. Chagneux, and S. Biggs, Soft Matter **7**, 2211 (2011).
[20] A. Zaccone, J. J. Crassous, B. Béri, and M. Ballauff, Phys. Rev. Lett. **107**, 168303 (2011).
[21] J. Malinge, F. Mousseau, D. Zanchi, G. Brun, C. Tribet, and E. Marie, J. Colloid Interface Sci. **461**, 50 (2016).
[22] M. Mani, A. Gopinath, and L. Mahadevan, Phys. Rev. Lett. **108**, 226104 (2012).
[23] H. Brenner, Chem. Eng. Sci. **16**, 242 (1961).
[24] M. E. O'Neill, Mathematika **11**, 67 (1964).
[25] A. J. Goldman, R. G. Cox, and H. Brenner, Chem. Eng. Sci. **22**, 637 (1967).
[26] W. B. Russel, D. A. Saville, and W. R. Schowalter, *Colloidal Dispersions* (Cambridge University Press, Cambridge, UK, 1989).
[27] H. Tu, L. Hong, S. M. Anthony, P. V. Braun, and S. Granick, Langmuir **23**, 2322 (2007).